Biomedical Engineering Advances 9 (2025) 100152

Contents lists available at ScienceDirect

Biomedical Engineering Advances

journal homepage: www.journals.elsevier.com/biomedical-engineering-advances

Decoding and generating synergy-based hand movements using electroencephalography during motor execution and motor imagery

Dingyi Pei, Ramana Vinjamuri *

Vinjamuri Lab, Department of Computer Science and Electrical Engineering, University of Maryland Baltimore County, Baltimore, MD, USA

ARTICLE INFO

Keywords:
Brain-machine interfaces
eeg
kinematic synergies
hand kinematics
motor imagery
motor execution

ABSTRACT

Brain-machine interfaces (BMIs) have proven valuable in motor control and rehabilitation. Motor imagery (MI) is a key tool for developing BMIs, particularly for individuals with impaired limb function. Motor planning and internal programming are hypothesized to be similar during motor execution (ME) and motor imagination. The anatomical and functional similarity between motor execution and motor imagery suggests that synergy-based movement generation can be achieved by extracting neural correlates of synergies or movement primitives from motor imagery. This study explored the feasibility of synergy-based hand movement generation using electroencephalogram (EEG) from imagined hand movements. Ten subjects participated in an experiment to imagine and execute hand movement tasks while their hand kinematics and neural activity were recorded. Hand kinematic synergies derived from executed movements were correlated with EEG spectral features to create a neural decoding model. This model was used to decode the weights of kinematic synergies from motor imagery EEG. These decoded weights were then combined with kinematic synergies to generate hand movements. As a result, the decoding model successfully predicted hand joint angular velocity patterns associated with grasping different objects. This adaptability demonstrates the model's ability to capture the motor control characteristics of ME and MI, advancing our understanding of MI-based neural decoding. The results hold promise for potential applications in noninvasive synergy-based neuromotor control and rehabilitation for populations with upper limb motor disabilities.

1. Introduction

Brain-machine interfaces (BMIs) show promising potential for enhancing the quality of life for those with upper limb paralysis. Recent years have witnessed significant progress in BMI technology, pushing the boundaries of motor control and rehabilitation. Research has shown the effectiveness of BMIs in restoring motor function to individuals with disabilities [1]. Furthermore, BMIs have proven valuable not only in motor control [2] but also in creating new avenues for recovering lost motor abilities and improving the overall quality of life for affected individuals [3]. Motor execution (ME) and motor imagery (MI) are two of the main paradigms that have emerged within the field of BMIs utilizing different neural processes. BMIs based on motor execution utilize neural signals produced during actual physical movements, decoding the brain's electrical activity when a person initiates and executes motor actions. In contrast, BMIs that rely on motor imagery detect and interpret brain signals associated with imagined movement patterns. This approach is particularly advantageous for individuals with motor impairments or disabilities, as it provides a means to regain mobility without requiring the physical execution of movements.

Over the past few decades, researchers have focused on developing MI-based BMIs for upper limb decoding. Substantial progress in the field of hand movement decoding of activities of daily living (ADL) has been achieved, especially in decoding motor imagery using non-invasive scalp EEG signals [4]. Many MI-based BMIs convert user intent into specific actions by recognizing event-related desynchronization (ERD) and event-related synchronization (ERS) from MI EEG. Agashe et al. decoded reach-to-grasp movements utilizing low-frequency EEG [5] and successfully implemented robotic hand control in individuals with amputation [6]. Research has shown that mu and beta frequency bands in EEG most effectively represent motor imagery [7], while EEG features extracted from spatial, spectral, and temporal domains have proven effective in distinguishing hand/wrist movements [8]. Significant classification accuracy was obtained by combining multi-dimensional features with a back propagation neural network, achieving 69 % accuracy for right-hand motor imagery tasks and 73 % for left-hand imagery tasks

* Corresponding author.
E-mail address: rvinjam1@umbc.edu (R. Vinjamuri).

https://doi.org/10.1016/j.bea.2025.100152
Received 5 December 2024; Received in revised form 10 February 2025; Accepted 20 February 2025
Available online 27 February 2025

[9]. The feature fusion network effectively mapped high-dimensional temporal-spectral features to a consolidated feature network, facilitating the discrimination and classification of right/left hand, feet, and tongue movements [10]. A novel multi-scale hybrid convolutional neural network was proposed for the decoding of cross-subject right/left hand imagery, yielding commendable performance [11].

However, the BMIs based on multiclass intention detection rely on the imagination of basic motor tasks. Except for the decoding of the left and right hands, feet, and tongue—where activation occurs in distinct areas of the motor cortex—detecting specific hand/finger movements using sensor-level EEG signals is challenging. This difficulty arises because precise hand movements, which involve different finger coordination, do not activate sufficiently distant regions to be effectively separated by the recording electrodes. [12]. Thus, the decoding of multidimensional hand movements from MI-based EEG is extremely challenging. Additionally, movement classification restricts the natural control of flexible and dexterous hand movements, preventing users from interacting with the environment based on dynamic and spontaneous intentions. Consequently, researchers have initiated efforts to decode the movement trajectories to achieve a more flexible and adaptable hand grasp by reconstructing the movement trajectories of upper limb movement from EEG signals [7,13]. Previous studies have shown the feasibility of predicting movement positions and velocities in the temporal domain [14,15]. Time-series neural activity can be linearly correlated to the speed of hand movements for both ME and MI [7,16,17] and can facilitate the prediction of upper limb movement trajectories [18–20]. However, it is challenging to map the correlations between time-series EEG with high-dimensional finger movements.

The larger number of degrees of freedom (DoFs) of the hand offers tremendous movement flexibility but also presents significant challenges for motor control. Challenge arises about how the central nervous system (CNS) effortlessly coordinates and modulates these DoFs and whether they are controlled independently or conjointly. To address this challenge of high dimensionality Nikolai Bernstein [21] proposed an idea of synergistic control which provides a theory of motor control that happens in a low-dimensional space of synergies. Synergies are described as a collection of multiple relatively independent motor units (DoFs) that are treated as a single functional element, which provides a spatiotemporal structure in movement coordination across both time as well as space of multiple DoFs [22]. With different combinations of a small set of synergies, several diverse hand movements can be reconstructed [23]. Studies in human sensorimotor control support the idea that the CNS simplifies the control of high DoFs and thereby reduces the complexity of motor control by using synergies [24–26]. Researchers have studied synergy-based BMIs to simplify modeling the complex relationships between high-dimensional brain activity and dexterous hand movements.

A synergy-based hand movement model [27] has been demonstrated, where hand kinematics (joint angular velocities) are represented as a weighted combination of kinematic synergies, containing both spatial and temporal characteristics of hand movements. The experimental evidence from human studies suggests that the hand grasp synergies can be decoded from invasive and non-invasive neural recordings [5,28,29]. These synergies have been demonstrated to offer insightful information for enhancing motor control and facilitating rehabilitation [30]. Synergy-based movement control leverages the natural coordination patterns of kinematics, facilitating more intuitive and coordinated movement restoration. For instance, a synergy-based movement model can help optimize BMI applications by reducing the dimensionality of control signals, making them easier to decode and execute. This could lead to more natural and efficient motor recovery compared to MI or ME-based approaches that rely on direct motor control without leveraging inherent kinematic coordination patterns. Previous studies also correlated the weights of hand kinematic synergies to neural spectral features captured during motor execution [31,32], offering a promising avenue for low-dimensional control using noninvasive EEG. Despite the fact that many neural control paradigms rely on motor imagery rather than motor execution, this is particularly advantageous for paralyzed individuals who cannot physically move. BMIs that are based on MI present a promising solution for these individuals.

It appears that ME and MI share brain control mechanisms, as evidenced by the temporal and spatial congruence between imagined and performed movements. It implies that both imagery and execution are produced by similar mechanisms, as both involve phases of planning and preparation prior to motor generation [33]. Thus, the motor planning/intention phase is also included in imagined movements. Unconscious motor preparation prior to execution and conscious motor imagery are thought to have similar mechanisms [34]. Besides the primary motor cortex [35], large overlapping brain regions and consistent activation in the cerebral cortex, including the premotor cortex, supplementary motor areas, prefrontal cortex, and inferior parietal cortex, are shared by both motor imagery and motor execution motor imagery and motor execution [36,37].

The functional equivalence between MI and ME provides a promising opportunity for synergy-based control based solely on MI without ME. In addition to the significant anatomical overlap between ME and MI [38], their spatiotemporal characteristics also suggest the similarity of functional correspondence between ME and MI [34,36,37]. Previous research has successfully decoded hand movements from EEG signals during motor execution using linear models [31,32,39,40]. This study seeks to investigate whether similar correlations exist between neural signals during motor imagery and hand kinematics, enabling the mapping and decoding of imagined hand movements. Furthermore, this study aimed to validate whether synergies derived from executed hand movements could be applied to generate imagined hand movements from MI EEG, ultimately enabling the development of assistive devices controlled by neural activity for individuals with impaired hand function.

2. Methodology

2.1. Experimental protocol

In this experiment, ten healthy, right-handed subjects (two females, average age 25.2 years, range 18–30 years) participated in this study. The participants were instructed to perform six hand grasp movements by reaching and grasping six objects selected from the activity of daily living (ADL). The selected objects (Fig. 1) are representative of six typical grasp types including cylindrical grasp (water bottle), hook grasp (door handle), lateral grasp (credit card), pinch grasp (screw), tripod grasp (screwdriver) and spherical grasp (ball). Prior to the experiment, the subject sat comfortably at a table with their dominant hand resting flat, palm down, on a designated starting point. The object was placed on the Table 30 cm away from the subject. The experiment includes two sessions, motor execution (ME) and motor imagery (MI). The process is shown in Fig. 2. In the ME session (Fig. 2(A)), the subject needs to perform a reach-grasp-hold hand movement under the instructions of the auditory cues. In the MI session (Fig. 2(B)), the subject was asked to imagine grasping the objects without any overt movements. In each session, a two-second period was given for movement preparation and another two seconds for execution/imagination. Subjects were instructed by the auditory cues to execute or imagine the grasping of objects. The objects were given in a random order and 30 repetitions were collected for each object. Between each session, 20 mins of break was provided.

2.2. Data collection

Data was collected under an approved protocol by the Internal Review Board (IRB, code 408) of the University of Maryland Baltimore County. During the experiment, hand joint angles were measured and

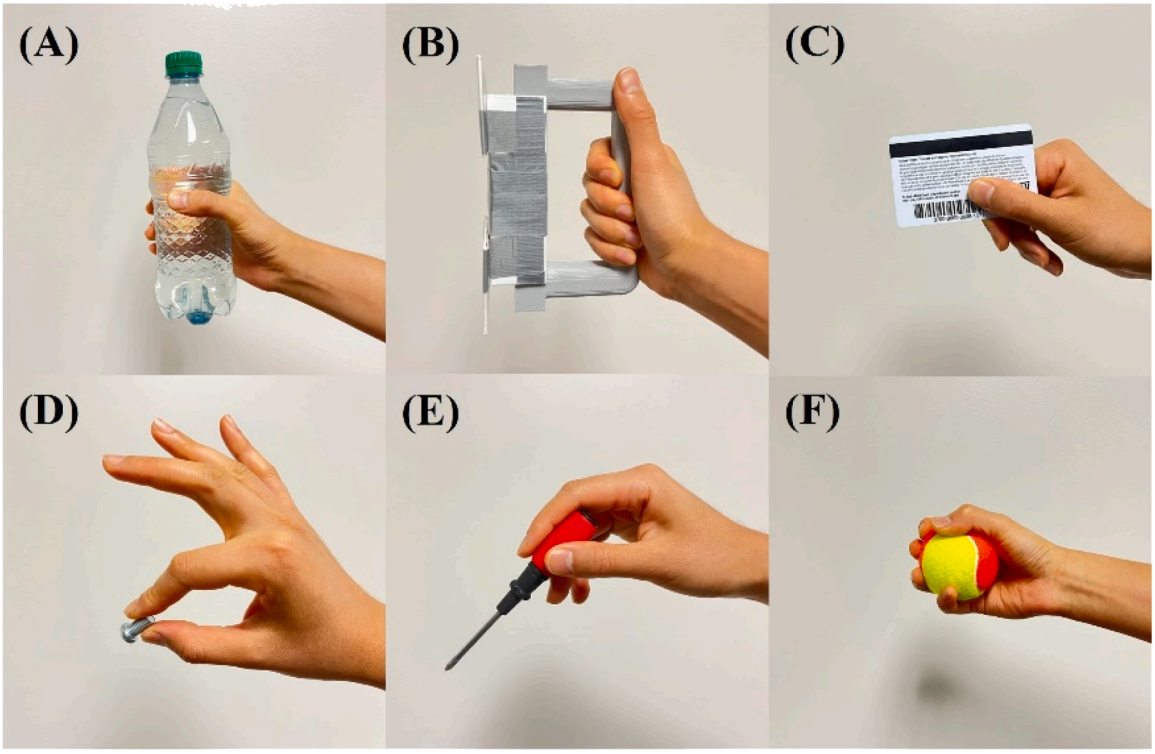

Fig. 1. Six object-grasp types: (A) cylindrical grasp (water bottle), (B) hook grasp (door handle), (C) lateral grasp (credit card), (D) pinch grasp (screw), (E) tripod grasp (screwdriver), (F) spherical grasp (ball).

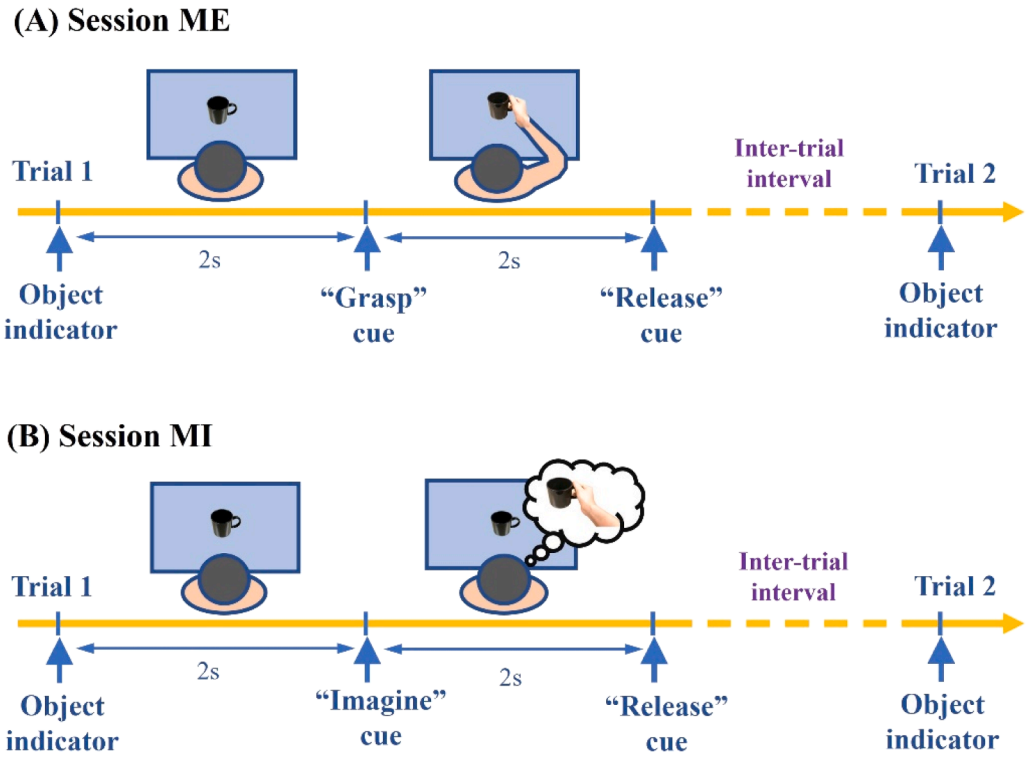

Fig. 2. Experimental protocol. (A) During motor execution, the subjects were asked to perform reach-grasp-hold hand movements guided by auditory cues. (B) During the motor imagery session, subjects were asked to imagine grasping the objects without any overt movements.

recorded with a CyberGlove (CyberGlove, CyberGloveSystems, San Jose, CA) at a 125 Hz sampling rate. Joint angles were recorded from 10 joint sensors of the CyberGlove corresponding to metacarpophalangeal (MCP) and interphalangeal (IP) joints of the thumb, and MCP and proximal interphalangeal (PIP) joints of four fingers respectively. EEG signals were captured with a high-density EEG cap. A total of 45

electrodes were selected and located on the motor-related areas spanning over the frontal (F), temporal (T), central (C) and parietal (P) areas. These electrode locations are Fz, F1, F2, F3, F4, F5, F6, F7, F8, FCz, FC1, FC2, FC3, FC4, FC5, FC6, FT7, FT8, Cz, C1, C2, C3, C4, C5, C6, T7, T8, CPz, CP1, CP2, CP3, CP4, CP5, CP6, TP7, TP8, Pz, P1, P2, P3, P4, P5, P6, P7, P8. The reference electrode was on the right or left ear lobe. Impedance was kept below 5 kOhms and checked throughout the experiment. Data were continuously captured by g.tec amplifier (g. HIamp, g.tec medical engineering GmbH, Graz Austria)) at a 600 Hz sampling rate. The 60 Hz power line frequency was digital notched. To ensure there was no motor-related activity in the upper limb, their forearm electromyography (EMG) was recorded by an 8-channel Delsys Trigno wireless EMG system (Delsys, MA United States) during the motor imagination. A custom-built Simulink (2020a, MathWorks, Inc. USA) model synchronized EEG system, CyberGlove and EMG system, and also provided auditory cues for action guidance. During the EEG signal recording, the subjects were instructed to minimize their eye-blinking and avoid swallowing/chewing during the 2-second data collection. Any artifacts detected by the instructor during the experiment led to immediate rejection and re-recording of those repetitions. A total of 32 repetitions were recorded for each type of movement in both ME and MI sessions. Recordings with hand movements extending beyond the 2-second period from the ME session and those with noticeable EMG signals during the MI session were eliminated. A maximum of two repetitions were discarded from each movement type. To maintain consistency, 30 repetitions were retained for each movement type across all subjects.

2.3. Derivation of kinematic synergies

The hand kinematics, or the joint angular velocities, recorded from the ME session were used to derive the hand kinematic synergies. The hand kinematics from ten joints were calculated from the differential of the recorded joint angles and the kinematic synergies were derived according to the synergy-based hand movement model [34]. As illustrated below:

$$v(t) = \sum_{j=1}^{n} w_j S^j(t) \tag{1}$$

The angular velocities $v(t)$ is expressed as a linear combination of synergies $S(t)$ and corresponding synergy weights w. To extract the synergies and the weights of the synergies, the hand kinematics were decomposed using value decomposition (SVD),

$$V = U\Sigma S = WS \tag{2}$$

V is the matrix of concatenated angular velocities of 10 joint angular velocities from all types of movements with dimensions m × *n*. S contains the eigenvectors, or principal components (PCs), which are considered as synergies. C is a matrix that contains weights assigned to synergy S. $\sum$ is a diagonal matrix (with diagonal values of $\lambda_1, \lambda_2, \ldots \lambda_n$) and Σ^2 represents the eigenvalues, which express the scale of the eigenvectors. Thus, the reconstructed angular velocities are represented as:

$$\widetilde{V} = U_k\{\lambda_1, \lambda_2, \ldots, \lambda_k\}S_k = WS_k \tag{3}$$

W is the weight matrix that consists of the coefficients of synergies. The top six synergies were selected based on the variance at a 95 % threshold.

$$\frac{{\lambda_1}^2 + {\lambda_2}^2 + \ldots + {\lambda_j}^2}{{\lambda_1}^2 + {\lambda_2}^2 + \ldots + {\lambda_n}^2} \geq 95\% \tag{4}$$

2.4. Neural representations of synergies

The raw EEG signals were first corrected by removing the global noises from each electrode using common average reference (CAR). Later, the signals were filtered to the 3–58 Hz range using a third-order Butterworth filter, effectively removing low-frequency artifacts (such as eye blinks and eye movements) as well as the 60 Hz power line interference. Then, the mean of the resting EEG signals—recorded at the beginning of the experiment as a baseline—was subtracted from the EEG signals. Prior EEG studies indicated that there is a significant modulation in sensorimotor rhythm (10–30 Hz) spectral power during both ME and MI of hand grasping [41], and individual finger movements can be decoded from mu (8–15 Hz) and beta (16–30 Hz) spectral features. Prior research successfully decoded synergy-based hand movements from 1 to 45 Hz spectral powers [31,32]. Another study focused on MI-based movement prediction has demonstrated that a combination of mu, beta, and gamma rhythms yields optimal results [42]. Thus, in this study, the neural decoding procedure was investigated by using multiple EEG rhythms inspired by prior research. A 4th order Butterworth filter was applied to filter the EEG signals into four frequency ranges, including 8–13 Hz (mu waves), 13–30 Hz (beta waves), 8–30 Hz (mu+beta), and 8–58 Hz (mu+beta+low gamma), which contain wide frequency components related to motor imagery.

The temporal-spectral features were extracted in this study to capture the dynamics of spectral changes of the EEG [13,42]. Each repetition a two-second period, and for each electrode, the EEG signals were segmented to half a second, forming a half-second sliding window with a 75 % overlap. The spectral power was then estimated from each segment window by calculating the band powers. The same procedure was repeated to all 45 EEG electrodes and all movements. The principal components were then extracted from all electrodes and all repetitions for each task using principal component analysis (PCA). Seven components explained 90 % of the variance were considered as neural features and the corresponding coefficients were considered as neural coefficients that were used to correlate with the weights of kinematic synergies. The flowchart of EEG analysis is illustrated in Fig. 3.

2.5. Neural decoding

Many studies suggested that rather than controlling each DoF independently, the CNS may employ synergies to reduce the complexity of motor control [24,25]. These studies indicate that synergies may be encoded in the CNS and can be used as an optimal control mechanism by the CNS in simplifying and achieving complex movements [26,43–46]. In this study, we hypothesize that since the synergies are the common patterns shared across a diversity of hand grasp movements, the brain may modulate the combinations of the synergies to regulate and generate the movements rather than forming synergies. Previous studies [14,40,47] revealed that each joint movement is independently regarded as a linear combination of neural activities in the time domain. Studies from [31,48] have successfully correlated neural activity with the weights of the synergies in ME movements.

After the neural coefficients were extracted from ME EEG signals, a linear multivariate regression model was applied to correlate the neural coefficients with corresponding hand kinematics weights.

$$w = c\beta \tag{5}$$

w contains the synergy weights, determined by kinematic synergy-based reconstruction. c is the neural coefficient matrix of a single task and β contains estimated model parameters. β was determined using the *mvregress* function in MATLAB 2022a. This function uses a maximum likelihood estimation to estimate, here, the diagonal elements of the variance-covariance matrix.

To evaluate the model's effectiveness and generalizability, it was validated both within and across all subjects.

2.5.1. Decoding within each subject

For each subject, among the ME movements, two-thirds of the

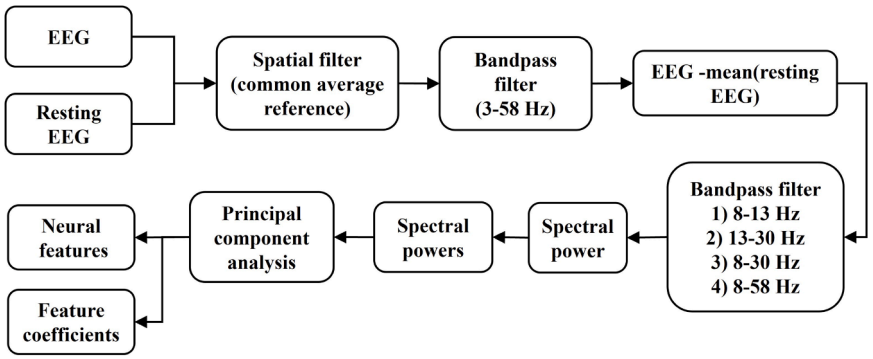

Fig. 3. The process of EEG processing and analysis.

repetitions in each task were selected to train a linear model for neural decoding, and the rest of one-third of the repetitions were used to test synergy-based reconstruction of hand kinematics. The performance was estimated using Pearson correlation coefficients between the recorded kinematics and decoded kinematics. To avoid bias from certain groups of training data, this model was evaluated with 10-fold cross-validation with shuffled repetitions in the training set and testing set in each fold.

As for the MI movement decoding, the neural coefficients were extracted using the same method as that used in ME EEG, and then neural coefficients were projected through the linear model developed by the ME movements to obtain the decoded synergy weights. After the synergy weights were decoded, the hand movements were generated by combining the MI synergy weights with ME kinematic synergies. The decoding paradigm is shown in Fig. 4. The collected neural and hand kinematics data were divided into training and testing sets for motor execution (ME) and motor imagery (MI), respectively. The ME training set was used to derive synergies and establish a linear correlation matrix between synergy weights and neural coefficients. In the MI testing set, the synergy weights for the MI group were decoded from their neural activity using the trained linear regression model. Decoded synergy weights were then combined with synergies to generate imagined hand movements. To evaluate the performance of neural decoding from MI, the decoded hand kinematics were compared with ME kinematics averaged across 30 repetitions for each task and within each subject. The decoding performance was compared between ME kinematics and MI kinematics. Decoding accuracy was measured using the Pearson correlation coefficient (ρ). The decoding error was defined as 1-$|\rho|$.

2.5.2. *Decoding across subjects*

To estimate the practicability of the neural correlation across the subjects, ten subjects were randomly divided into training set (nine subjects) and testing set (one subject). Although the synergies vary across different individuals depending on their own unique movement primitives, previous studies have shown [49,50] that spatiotemporal patterns of synergies are not only shared across a different set of motor behaviors but also carry generalized control strategies across individuals. Hence, in this part, the hand kinematics were derived from movements recorded from the training set, and kinematic synergies were extracted from all types of hand grasps across subjects according to the synergy-based hand movement model. Subsequently, the model was employed to predict imagined movements for the remaining subject based on MI signals. To ensure robustness, a 10-fold cross-validation approach was employed in this analysis.

3. Results

The kinematic synergies and neural decoding model were derived from ME data. These models were then applied to decode hand kinematics from both ME and MI EEGs achieving a decoding accuracy of up to 89.7 % for ME and 95.5 % for MI across all movement tasks and all

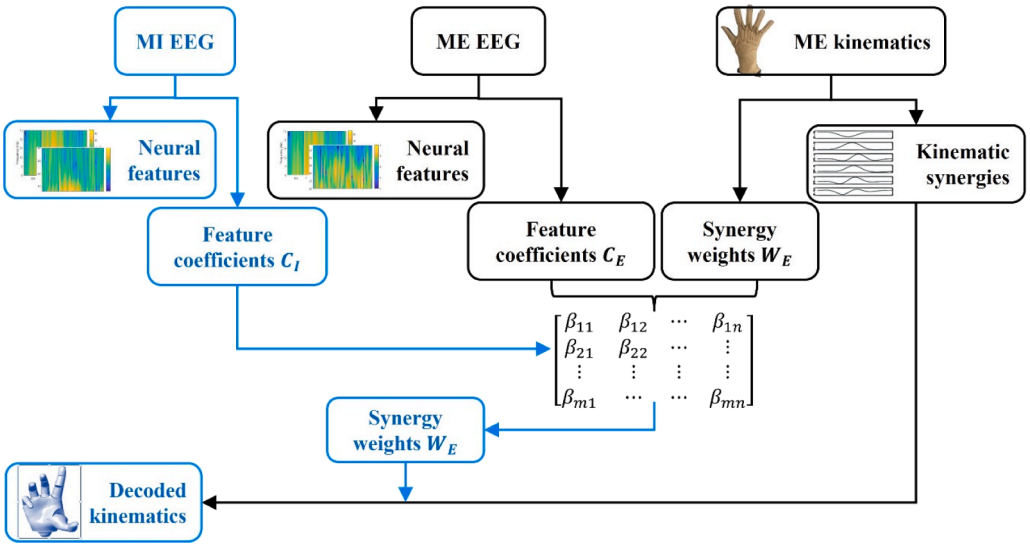

Fig. 4. The interpretation of MI-based hand kinematics (represented in blue) was achieved through a linear regression model constructed from ME (illustrated in black). The neural features and associated coefficients were extracted from the principal components of all EEG electrodes for each task. The weights of synergies from MI were calculated using corresponding neural coefficients through this multivariate linear regression model, and the hand kinematics were then decoded by linearly combining the decoded synergy weights and the kinematic synergies.

individuals. The decoding accuracy of ME movement was measured by comparing the correlations between the recorded kinematics and neural decoded kinematics. As for MI-based decoding, the decoded hand kinematics was compared with the mean of ME kinematics across all repetitions. Table 1 presents the decoding accuracy results for ME and MI across various EEG frequency bands, illustrating the average performance across the six movement tasks. The results show that no significant difference was observed in the decoding accuracy from ME when using four bandwidths of EEG waves, while the performance of MI differs across different EEG rhythms observed from most of the subjects ($p < 0.05$). MI decoding from beta waves (13–30 Hz) performed the best in general among different EEG rhythms. The commonly considered EEG frequency range for MI, 8–30 Hz, demonstrated slightly lower accuracy when compared with the beta band and the broader 8–58 Hz band. Surprisingly, the mu rhythm (8–13 Hz) displayed the lowest decoding accuracy when compared to other frequency bands.

Fig. 5 shows the spectrogram of ME and MI EEG during the movement execution and imagery, compared with resting EEGs. Within the 8–30 Hz frequency range, clear synchronization and desynchronization patterns emerge in both ME and MI EEGs, both before and during the execution or imagination of movements. However, the spectral power observed in MI EEGs appears to be weaker than that in ME EEGs. This observation suggests that the relatively weaker spectral power in MI EEG signals might hinder the decoding performance when relying solely on mu wave activity, emphasizing the importance of considering additional neural representations for more robust decoding outcomes.

Fig. 6 provides averaged MI-based decoding errors for each joint and grasp type averaged from all subjects using the frequency band of 13–30 Hz of MI-based EEG. Generally, thumb, index and middle play prominent roles in various grasping actions, and as a result, decoding performance exhibits variability across different grasp types. As illustrated in Fig. 6, we observe that decoding errors tend to be higher for the thumb and index finger joints compared to other joints. However, the performance of the ring and pinky fingers remains remarkably stable and consistent across distinct movements, which may be due to the fact that these two fingers have more freedom in grasping. Our analysis reveals that distinct grasp types can significantly influence decoding outcomes. For example, in the case of the lateral grasp (where the object being grasped is a credit card), it's not surprising to find that the middle, ring, and pinky fingers exhibit the lowest error rates across all finger joints and grasp types. This result aligns with the functional roles of these fingers in executing lateral grasps effectively. Also, the pinch grasp demands a higher degree of precision and delicate motor skills, posing challenges in maintaining consistent performance each time this grasp is used, particularly when relying on the thumb and index fingers. Therefore, these two dominant fingers tend to have the highest error rates in decoding, reflecting the intricate nature of pinch grasping movements.

Fig. 7 provides the comparison between the average recorded kinematics from ME and decoded kinematic patterns from MI specifically focusing on the thumb, index, and middle fingers. It is predictable that there is variability in performance across individuals. Among all six types of grasps, for Subject 1, the corresponding kinematic trajectories of key digits decoded from MI EEGs were predicted accurately especially in cylindrical grasps (using a water bottle as the object) and pinch grasp (utilizing a screw as the object).

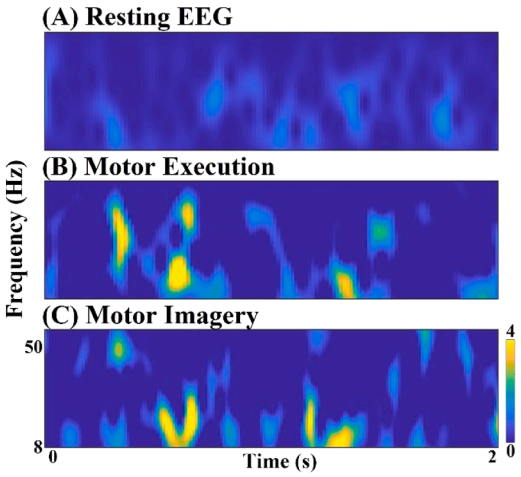

Fig. 5. Spectrograms of EEG for resting, motor execution and motor imagery. Compared with resting states of EEG signals, clear synchronization and desynchronization before and during the execution/imagery can be observed from ME and MI EEG.

Fig. 8 presents a detailed visualization of the decoded kinematics of a cylindrical grasp for ten joints. Results show the averaged trajectories across 30 repetitions represented by solid lines, with standard deviation across repetitions indicated by shaded areas. The decoding model exhibited the ability to adjust weights uniquely for different movements, thus enabling the successful decoding of diverse angular velocity patterns associated with different objects.

Fig. 9 illustrates the topographies of spatial representations of neural coefficients extracted from the beta waves for both ME and MI across all subjects and tasks, providing a clear view to interpret the possibility of neural decoding of MI based on ME. The neural feature coefficients were extracted using PCA and the top three principal components were considered as neural features, and the corresponding weights of each component were considered as the neural coefficients used to correlate with weights of hand kinematic synergies. Generally, the spectral coefficient of ME is greater than MI. From Fig. 9, it can be observed that the first coefficient in both ME and MI shares common structural patterns among various tasks. The first coefficient in both ME and MI shares common structural patterns among various tasks. Significant coefficients were found bilaterally in the primary motor (M1), premotor and somatosensory cortices. The second coefficients show differences, with ME distributions extending from the superior to the inferior side of motor-related regions, while MI distributions are more concentrated around the supplementary motor area. It can be observed that the same activation that greater neural activation was found from the supplementary motor area (SMA) and pre-supplementary motor area (preSMA)

Table 1
Accuracy of individual neural decoding of ME and MI across each frequency band.

Subject #		1	2	3	4	5	6	7	8	9	10	Mean ± Std
ME	8–13Hz	94.5	86.6	93.9	93.6	94.4	68.5	92.8	87.5	85.4	94.4	89.2 ± 8.1
	13–30Hz	95.0	86.7	94.5	93.9	94.7	69.7	93.0	86.6	88.8	93.6	89.7 ± 8.6
	8–30Hz	94.7	86.2	94.9	93.4	94.6	70.3	93.4	86.8	87.7	93.8	89.5 ± 7.6
	8–58Hz	94.5	86.4	93.9	93.6	94.7	71.3	93.7	86.5	83.1	92.4	89.0 ± 7.5
MI	8–13Hz	96.1	58.0	93.3	65.4	32.2	83.9	31.5	55.7	57.9	66.0	64.0 ± 22.4
	13–30Hz	97.8	92.9	98.1	94.6	97.8	90.6	97.3	95.4	93.5	96.9	95.5 ± 2.5
	8–30Hz	98.7	93.2	98.5	95.4	62.2	89.7	92.8	89.9	91.5	95.9	90.8 ± 9.5
	8–58Hz	98.2	93.1	97.9	95.7	96.5	89.1	95.4	95.9	93.8	92.8	94.8 ± 2.7
			*		*	*		*	*	*	*	

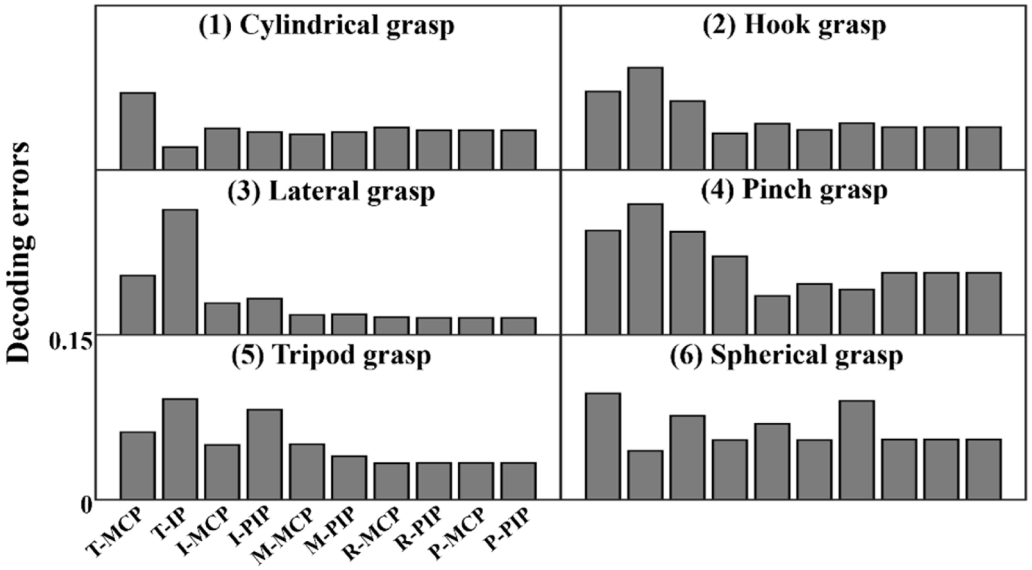

Fig. 6. Decoding errors of ten joints for six types of grasp tasks averaged for all subjects using beta rhythms of MI EEG signals. Among all six tasks, the thumb and index hold relatively higher decoding errors compared to the rest of the three fingers, especially in the tasks that need more precision operation using the thumb and index including lateral, pinch and tripod grasps. T: thumb, I: index, M: middle, R: ring, P: pinky. MCP: Metacarpophalangeal joint, IP: Interphalangeal joint, PIP: Proximal interphalangeal joint.

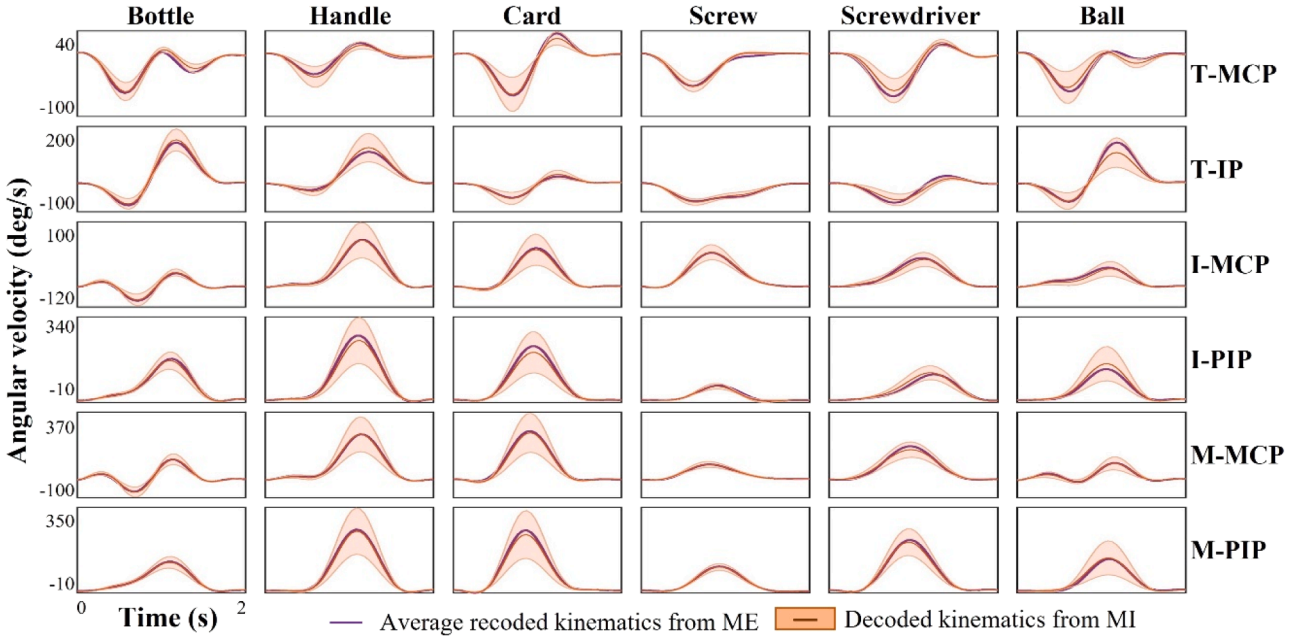

Fig. 7. Hand joint angular velocities of six types of grasps and joints from thumb, index and middle. The recorded kinematics from ME (in black) were averaged across all repetitions from each task and compared to the neural decoded kinematics (in red) from Subject 1, band 13–30 Hz. The standard deviations are represented by the shaded regions. The ring and pinky fingers are not shown for simplicity. T: thumb, I: index, M: middle, R: ring, P: pinky. MCP: Metacarpophalangeal joint, IP: Interphalangeal joint, PIP: Proximal interphalangeal joint.

in MI versus ME. The dominant variance between ME and MI can be found in the third coefficient, where the ME distributions were more concentrated in the central motor area and MI distributions were separated from temporal to the central area across different movement tasks.

To decode hand kinematics across individuals, we first derived kinematic synergies and developed a neural decoding model using a training set. Then, for the testing set, we calculated the synergy weights to decode the hand kinematics. The hand kinematics were successfully reconstructed from neural representations with an average decoding accuracy of 70.8 ± 5.5 % across all movement tasks and all individuals in randomly selected subgroups of subjects. Compared with the individual movement decoding, the decoded joint velocity trajectories across all individuals yielded better performance using their own decoding model and kinematic synergies, with an average 70.2 % correlation compared to recorded kinematics from the ME session. The snapshots of recorded and decoded hand postures taken from discrete time points in the progression of a grasp are shown in Fig. 10. While finger movement trajectories may not be exactly identical to recorded movements when using decoding across individuals, the end-posture of the hand tripod grasp demonstrates a high degree of similarity between

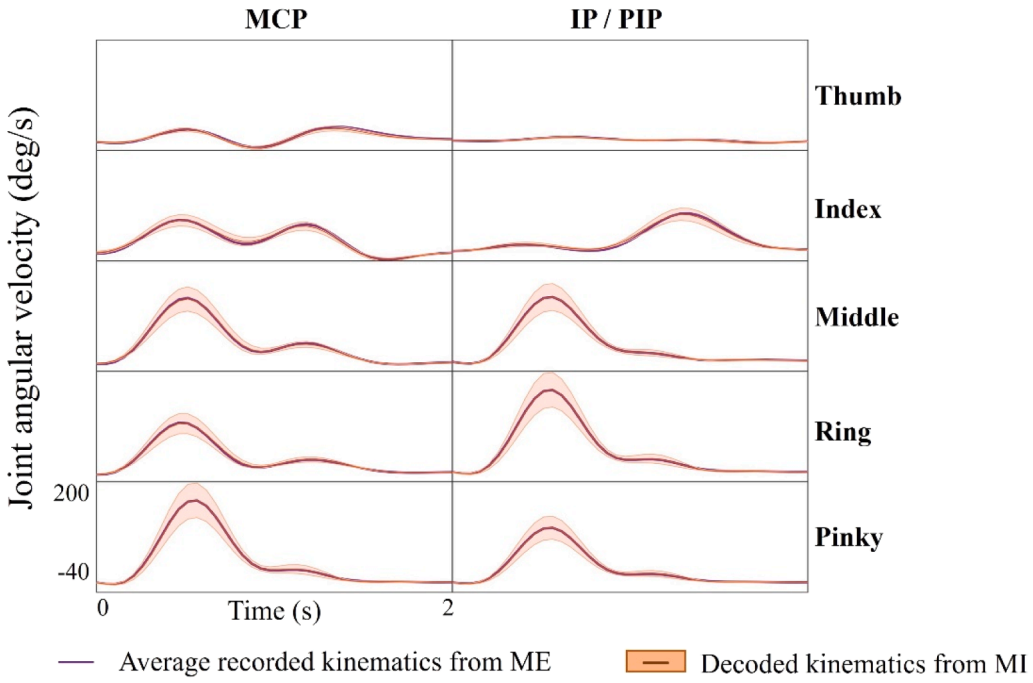

Fig. 8. Decoding hand kinematics of cylindrical grasp for 10 joints (Subject 1, beta (13–80 Hz)). The recorded kinematics (in black) was averaged across all repetitions to compare with the neural decoded kinematics (in red) and the shaded regions represent standard deviations of all MI repetitions.

recorded and decoded movements.

4. Discussion

This paper demonstrated a hand synergy-based neural decoding model using motor imagery for dynamic hand kinematic trajectory decoding. The model translates neural representations into synergy weights and thereby generating dexterous hand kinematics from MI-based neural features. This supports potential applications of non-invasive synergy-based BMIs in neuro-motor control and rehabilitation of individuals with upper limb motor deficits.

4.1. Decoding hand trajectory from motor imagery using synergy-based models

From the results obtained, decoding accuracy was up to 89.7 % for ME and 95.5 % for MI across all tasks and individuals. Since the decoding model was created and trained using ME signals along with corresponding hand movements, its performance is expected to be better with ME-based EEG than with MI-based EEG. In the case of MI, the decoding performance was determined by comparing the results with the averaged ME kinematics across all repetitions. To compare ME and MI, we also calculated ME decoding accuracy by correlating the decoded movements with the averaged recorded movements across repetitions. The results showed an average accuracy of 96.8 $\pm$ 5.3 %, 96.7 $\pm$ 5.4 %, 96.7 $\pm$ 5.4 %, and 96.9 $\pm$ 4.7 % for each frequency band. Higher accuracies were observed compared to MI decoding (Table 1).

Decoding dexterous hand movements is challenging due to the involvement of multiple degrees of freedom (finger joints) and their temporal variability. Prior research primarily focused on discrete movement classification of end postures [51,52]. This method has limitations, as individuals may grasp similar objects with similar end postures but vary in their hand kinematics. Our model aims to replicate the natural movements by mapping the user intent to hand movement trajectories, preserving spatial and temporal characteristics [53]. Few studies have focused on decoding full kinematic movement trajectories. Agashe et al. developed a finger movement decoder that mapped brain signals to joint angles in the time domain to generate joint angle trajectories [40]. However, each movement variable was modeled independently, achieving up to 76 % similarity between the predicted and observed trajectories. Another study demonstrated that powers of mu and beta rhythms are linearly related to hand movement velocities of right/left hand clenching [54] with an average of 74 % of hand prediction and 32 % of velocity decoding. Lv Jun et al. decoded hand movement speed during drawing tasks and reached an average of 37 % decoding accuracy on a single axis in 2-dimensional space [16]. Compared to the previous studies, our approach offers a simplified model based on synergies for improved performance.

In contrast to the conventional approach of directly correlating neural representations with hand movement trajectories, our study hypothesizes that the CNS may regulate various movements by modulating the combinations of the synergies. The functional equivalence between MI and ME provides an opportunity for synergy-based control using MI-based EEG. The correlations between neural coefficients and synergy weights established in this study demonstrate the feasibility of simplifying the MI-based neural decoding of movement trajectories. Some studies proposed that movement parameters such as position, velocity, and movement direction are most effectively decoded from low-frequency time-domain signals [14,15]. Movement speed decoding study found that the 20–28 Hz frequency band carried the most notable information [16]. In studies that predict upper limb movement trajectories, mu and beta band activity (8–30 Hz) have been extensively used to classify and reconstruct both executed and imagined movement trajectories, offering superior performance compared to other brain rhythms [7,17–20]. Of the four frequency bands examined in this study, beta waves (13–30 Hz) and broad-spectrum EEG activity (8–58 Hz) were the most promising for MI-based decoding.

4.2. Neural decoding based on motor execution and motor imagery

While mu and beta waves are primary rhythms commonly associated with motor imagery, with optimal performance often observed in the 8–30 Hz range, this study found that beta waves consistently outperform other rhythms in MI-based movement decoding. Mu waves yielded the lowest decoding accuracy compared to other frequency bands, with MI-based decoding failures occurring in 7 out of 10 subjects (Table 1). In

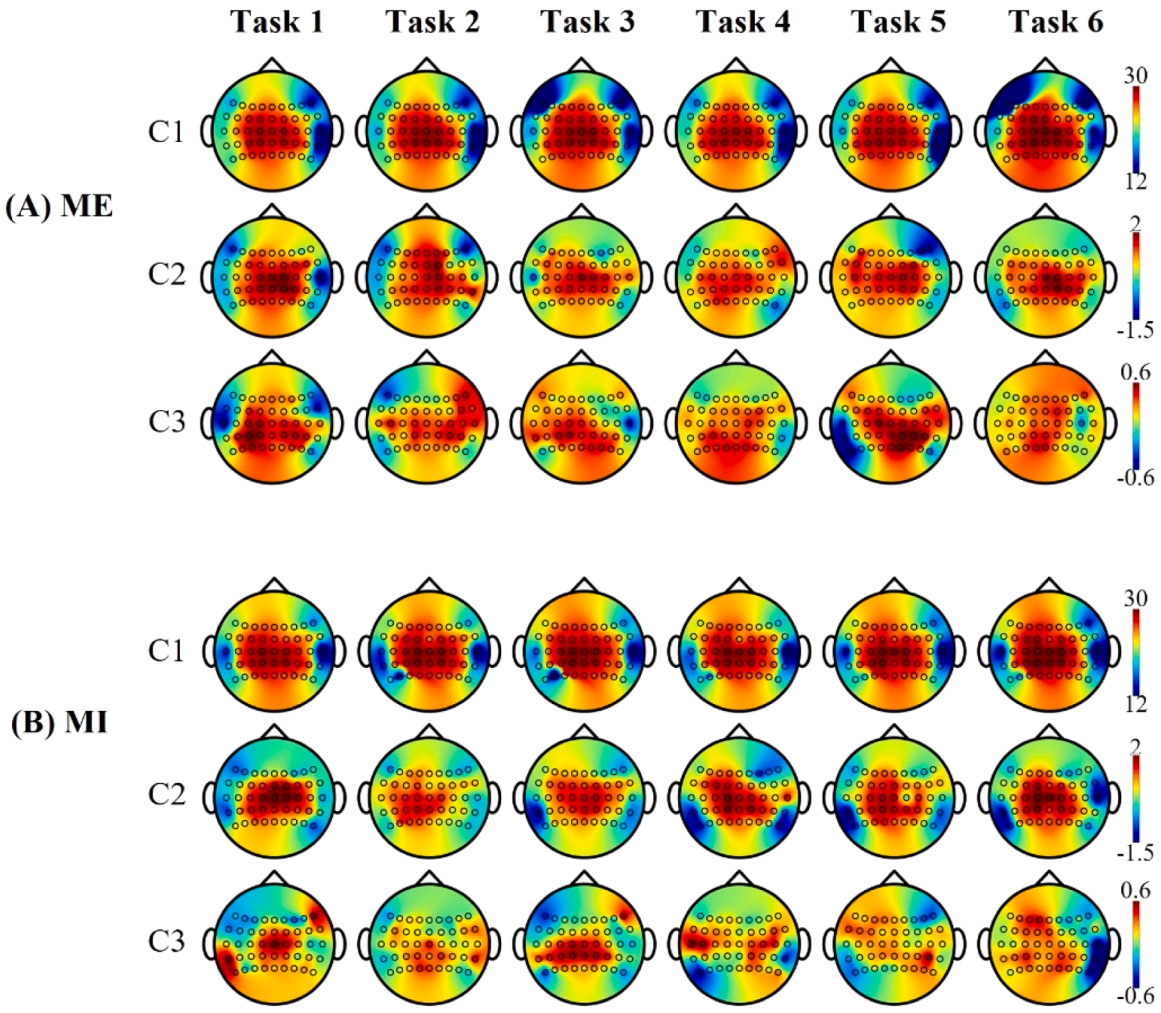

Fig. 9. Topographies of spatial representations of neural coefficients of beta waves from ME-based and MI-based principal components for six different grasping tasks. The top three principal component coefficients extracted from EEG activity were correlated with the weights of hand kinematic synergies. The first coefficient in both ME and MI exhibits common structural patterns across various tasks while the second coefficient shows distinct differences, with ME distributions extending from the superior to the inferior regions of motor-related areas, and MI distributions are more localized around the supplementary motor area. ME distributions of the third coefficient are more concentrated in the central motor area, while MI distributions vary across different movement tasks.

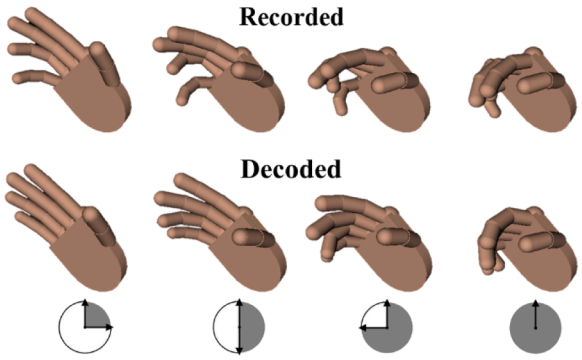

Fig. 10. The snapshots of recorded and decoded hand postures taken at discrete time points in the progression of a grasp (Task 5, tripod grasp, object of a screwdriver, from subject 4). The finger movements are not perfectly identical between the recorded and decoded movements when decoding across individuals. The end-posture of the hand tripod grasp demonstrates a high degree of similarity between recorded and decoded movements.

contrast, ME-based decoding across various EEG rhythms demonstrated relatively consistent performance levels. These findings highlight the distinct neural mechanisms underlying motor execution and motor imagery, which likely contribute to the observed differences in decoding outcomes using mu and beta rhythms.

While some beta rhythms have been linked to mu rhythms, others operate independently, each with unique topographical distributions and roles in motor function [55,56]. Studies have revealed that the distinction between motor execution and imagery extends beyond power spectra and topographies, as evidenced by individual differences in mu rhythm responses during movement-related tasks [55]. Moreover, some studies have shown significant contralateral suppression in beta rhythms compared to mu rhythms [57]. These factors may contribute to the observed disparities in decoding performance between ME and MI, particularly the relatively poor MI-based decoding results in most subjects in this study. This also highlights the potential for inter-individual variability in neural activation during motor imagery, posing additional challenges for achieving generalized neural decoding across diverse individuals.

Fig. 9 illustrates the significant overlap in neural activations between ME and MI, primarily within motor-related regions. However, subtle distinctions arise in the second coefficients, with ME distributions extending from the superior to inferior regions of the premotor cortex,

primary motor cortex, and primary somatosensory cortex. In contrast, MI distributions are more concentrated in the supplementary motor area, superior primary motor cortex, and superior primary somatosensory cortex. These findings align with fMRI studies [58,59], hat reported greater neural activation in the supplementary motor area (SMA) and pre-supplementary motor area (preSMA) during MI compared to ME, suggesting a role in motor-related cognitive control. Moreover, significant involvement of the SMA has been identified in movement decoding from ME [15] and MI [60].

4.3. Challenges and opportunities for synergy-based models based on motor imagery

This study explored neural decoding both within and across individuals. For individual decoding, neural activity was correlated with each person's unique kinematic synergies to reconstruct their movements. However, predicting hand kinematics from MI signals in individuals with paralysis, such as stroke patients, poses challenges due to the difficulty in deriving synergies and correlating MI signals with specific movements, especially for dynamic trajectories. To address this, the study preliminarily investigated a linear neural decoding model combined with a synergy-based movement model. This approach compensated for missing hand kinematic synergies by using those derived from healthy individuals, assuming a common correlation between brain activity and hand synergies across groups. Previous studies by us and others suggested that synergies might be shared across various motor behaviors and represent generalized control strategies [32,49,50]. However, this study found that decoding performance was lower across individuals (average accuracy of 70.8 %) compared to within individuals (average accuracy of 95.5 %). While the linear neural decoding model effectively linked neural activity with hand synergies within individuals, improving its generalizability for decoding MI signals across individuals, especially those with upper limb mobility impairments, remains an area for further research. The successful decoding of MI hand movements using correlations from ME supports the hypothesis that fundamental neural circuits underlying movement execution share common synergies. Future research could focus on refining the correlation model by extracting more informative neural features from EEG signals and developing more robust decoding models. Additionally, investigating the generalizability of the neural decoding model across different individuals is crucial for practical applications.

Individual variability in motor primitives employed during similar grasps can contribute to differing synergy patterns, as illustrated in Fig. 11, where the first three synergies account for at least 85 % of the variance. While the first synergy postures are similar across individuals, the second and third synergies demonstrate differences across individuals, highlighting the role of unique primitives in movement formation. Recent studies suggest that a limited number of hand synergies are shared across movements [61] and are influenced by movement speed [62]. Therefore, subject-specific synergies may provide more accurate representations and performance compared to synergies extracted across subjects [63]. Moreover, literature suggested that the variability among different individuals influences neuromuscular control. Factors such as age have been shown to affect muscle synergy complexity and efficiency, and muscle synergy metrics can be affected by cognitive and postural constraints [64]. Macchi et al. [65] revealed clear gender-related differences in the lower limb activities and muscle synergies during the training process. These individual variabilities contribute to motor dexterity and influence movement generation when employing non-subject-specific synergies. However, the extent to which factors such as age, sex, and hand dominance impact hand synergy formation and neural decoding remains unclear and requires further investigation. To develop more generalized decoding models, future studies should incorporate a more diverse cohort and increased sample size, ensuring the robustness of synergy-based approaches for individuals with motor impairments. Furthermore, future research will explore the selection of appropriate hand movements, individual group, and analytical methods for constructing effective MI-based decoding models that can be generalized across individuals.

4.4. Potential applications and challenges of the proposed models in individuals with stroke

The results from this study suggest that the CNS may regulate different combinations of synergies to achieve various hand grasps, and the weights of these synergies might be encoded in the higher-level neural systems. This synergy-based movement control allows for the modulation of synergy weights enabling diver grasps without controlling at the level of individual joints. This provides an alternative potential application in terms of rehabilitation for individuals with motor deficits such as those recovering from a stroke. Different from current BMI-based rehabilitation methods, which focus on decoding users' movement intentions, synergy-based BMIs can restore dynamic and natural movement patterns with fewer control units, enabling more active motor control during the rehabilitation process. Additionally, synergy-based BMIs could be integrated with robotic exoskeletons to assist in motor retraining for stroke survivors and individuals with spinal cord injuries, ensuring that rehabilitative movements more closely resemble natural motor patterns, or align with the brain's intrinsic motor control strategies, ultimately improving overall performance. To achieve this, understanding the role of non-subject-specific synergies derived from healthy individuals is crucial for compensating for the restoration of hand kinematics in individuals with motor impairments, which is discussed in Section 4.3.

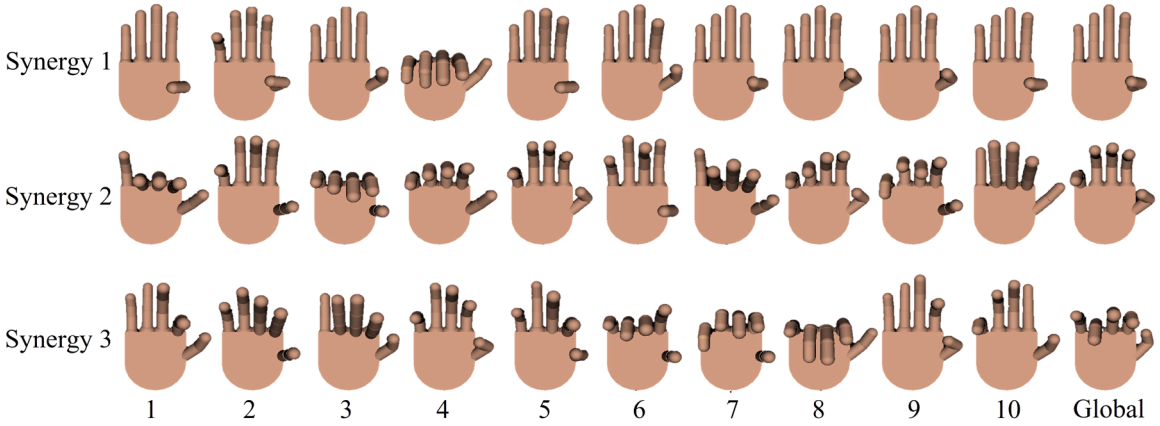

Fig. 11. Top three synergy postures of ten subjects. Within each postural synergy, the difference among individuals represents a subject-specific preference for synergy recruitment.

When considering the application of BMIs for individuals with stroke, a significant challenge arises due to abnormalities in cortical rhythms in motor-related brain regions [66–68]. Individuals with contralateral hemiparesis often experience impaired finger mobility and dexterity, hindering voluntary motor movements [69]. The suppression of sensorimotor rhythms in individuals with stroke could potentially impact the decoding accuracy of BMIs. Our findings suggest that beta waves (13–30 Hz) outperform other EEG rhythms in MI-based movement decoding. The shared computational mechanisms underlying ME and MI are essential for decoding imagined movements using ME-trained neural decoding models. However, abnormal EEGs and impaired upper limb mobility often seen in individuals with stroke could significantly limit the applicability of our model.

Prior studies suggest that compared to healthy individuals, motor cortical activations are higher in those with moderate motor deficits but may be diminished or absent in severely affected patients attempting to move their affected hands [67]. During imagined finger movements, increased beta wave connectivity (13–30 Hz) has been observed linking the contralateral primary motor area, premotor area, and primary sensory area, compared to overt movements [70]. Research on stroke-related ME and MI has demonstrated a higher contralesional event-related desynchronization (ERD) and a stronger ipsilesional event-related synchronization (ERS) in individuals with more severe impairments compared to those with milder ones [71]. Also, in individuals who have suffered stroke studies showed reduced ability to decode hand movements using movement-related cortical potential compared to healthy individuals [72]. These findings highlight the potential challenges in developing a robust and effective BMI system for stroke patients, particularly given the changes in the contralesional hemisphere. While some studies have demonstrated the potential of MI-based BMIs to predict hand movements from MI EEG signals in individuals with stroke [10,11,73,74] and enhance performance after training [75], particularly with bi-hemispheric beta activity [76], further research is needed to determine the applicability of our neural decoding model. Understanding how changes in rhythms influence synergy modulation among the stroke population is crucial. The ability to accurately and efficiently decode motor imagery hand movements could not only enhance the usability and effectiveness of MI-based BMI systems but also play a vital role in rehabilitating patients with cerebral motor impairments through the use of BMI-assisted devices.

5. Conclusion

This study developed a synergy-based model that successfully decoded hand movement trajectories from neural activity during motor imagery. This paradigm is promising for individuals with motor impairments, as it offers an alternative pathway for motor function restoration and has the potential to improve their quality of life. Understanding the functional relationships between motor execution and motor imagery might give rise to new approaches for motor control and rehabilitation. By capturing neural correlates of synergies, BMIs could extend beyond intention decoding and provide intuitive control of assistive robotics and exoskeletons. Furthermore, the high decoding accuracies achieved in this study using various EEG rhythms suggest the potential for decoding hand movements through noninvasive cortical activities, opening doors for dexterous hand movement decoding in individuals with stroke.

Conflicts of interest

The authors declare no conflict of interest.

CRediT authorship contribution statement

Dingyi Pei: Writing – review & editing, Writing – original draft, Validation, Software, Formal analysis, Data curation, Conceptualization.

Ramana Vinjamuri: Writing – review & editing, Writing – original draft, Supervision, Resources, Project administration, Methodology, Investigation, Funding acquisition, Conceptualization.

Declaration of competing interest

The authors declare that they have no known competing financial interests or personal relationships that could have appeared to influence the work reported in this paper.

Acknowledgments

This research was funded by the National Science Foundation (NSF) CAREER Award, grant number IIS-2053498 and NSF IUCRC Phase II UMBC: BRAIN, grant number CNS-2333292.

Data availability

Data will be made available on request.

References

[1] M.A. Khan, R. Das, H.K. Iversen, S. Puthusserypady, Review on motor imagery based BCI systems for upper limb post-stroke neurorehabilitation: from designing to application, Comput. Biol. Med. 123 (2020).
[2] L. Tonin, J. del R. Millán, Noninvasive brain–machine interfaces for robotic devices, Annu. Rev. Control. Robot. 4 (2021) 191–214.
[3] R. Mane, T. Chouhan, C. Guan, BCI for stroke rehabilitation: motor and beyond, J. Neural Eng. 17 (2020), https://doi.org/10.1088/1741-2552/aba162.
[4] G.R. Müller-Putz, A. Schwarz, J. Pereira, P. Ofner, From classic motor imagery to complex movement intention decoding: the noninvasive Graz-BCI approach, Prog. Brain Res. 228 (2016) 39–70, https://doi.org/10.1016/bs.pbr.2016.04.017.
[5] H.A. Agashe, A.Y. Paek, Y. Zhang, E.W. Sellers, Global cortical activity predicts shape of hand during grasping, Front. Neurosci. 9 (2015) 121, https://doi.org/10.3389/fnins.2015.00121.
[6] H.A. Agashe, A.Y. Paek, J.L. Contreras-Vidal, Multisession, Noninvasive Closed-Loop Neuroprosthetic Control of Grasping By Upper Limb Amputees, 1st ed., Elsevier B.V., 2016 https://doi.org/10.1016/bs.pbr.2016.04.016.
[7] A. Korik, R. Sosnik, N. Siddique, D. Coyle, Imagined 3D hand movement trajectory decoding from sensorimotor EEG rhythms, in: 2016 IEEE Int. Conf. Syst. Man, Cybern. SMC 2016 - Conf. Proc, 2017, pp. 4591–4596, https://doi.org/10.1109/SMC.2016.7844955.
[8] S.-B. Lee, H.-J. Kim, H. Kim, J.-H. Jeong, S.-W. Lee, D.-J. Kim, Comparative analysis of features extracted from EEG spatial, spectral and temporal domains for binary and multiclass motor imagery classification, Inf. Sci. (Ny). 502 (2019) 190–200.
[9] A. Sivakami, S.S. Devi, Analysis of EEG for motor imagery based classification of hand activities, Int. J. Biomed. Eng. Sci. 2 (2015) 11–22.
[10] Y. Li, L. Guo, Y. Liu, J. Liu, F. Meng, A temporal-spectral-based squeeze-and-excitation feature fusion network for motor imagery EEG decoding, IEEE Trans. Neural Syst. Rehabil. Eng. 29 (2021) 1534–1545, https://doi.org/10.1109/TNSRE.2021.3099908.
[11] X. Tang, C. Yang, X. Sun, M. Zou, H. Wang, Motor imagery EEG decoding based on Multi-scale hybrid networks and feature enhancement, IEEE Trans. Neural Syst. Rehabil. Eng. 31 (2023) 1208–1218, https://doi.org/10.1109/TNSRE.2023.3242280.
[12] M.H. Schieber, Motor cortex and the distributed anatomy of finger movements, Adv. Exp. Med. Biol. 508 (2002) 1–6.
[13] A. Korik, R. Sosnik, N. Siddique, D. Coyle, Decoding imagined 3D hand movement trajectories from EEG : evidence to support the use of mu, beta, and low gamma oscillations, Front. Neurosci. 12 (2018) 1–16, https://doi.org/10.3389/fnins.2018.00130.
[14] J.M. Antelis, L. Montesano, A. Ramos-murguialday, N. Birbaumer, J. Minguez, On the usage of linear regression models to reconstruct limb kinematics from low frequency EEG signals, PLoS. One 8 (2013) e61976, https://doi.org/10.1371/journal.pone.0061976.
[15] P. Ofner, G.R. Muller-Putz, Movement target decoding from EEG and the corresponding discriminative sources: a preliminary study, Proc. Annu. Int. Conf. IEEE Eng. Med. Biol. Soc. EMBS (2015) 1468–1471, https://doi.org/10.1109/EMBC.2015.7318647, 2015-Novem.
[16] J. Lv, Y. Li, Z. Gu, Decoding hand movement velocity from electroencephalogram signals during a drawing task, Biomed. Eng. Online. 9 (2010) 64, https://doi.org/10.1186/1475-925X-9-64.
[17] N. Robinson, A.P. Vinod, C. Guan, Hand movement trajectory reconstruction from EEG for brain-computer interface systems, in: Proc. - 2013 IEEE Int. Conf. Syst. Man, Cybern. SMC 2013, 2013, pp. 3127–3132, https://doi.org/10.1109/SMC.2013.533.
[18] A. Korik, R. Sosnik, N. Siddique, D. Coyle, 3D hand motion trajectory prediction from EEG mu and beta bandpower, Prog. Brain Res. 228 (2016) 71–105.

[19] A. Korik, R. Sosnik, N. Siddique, D. Coyle, EEG mu and beta bandpower encodes information for 3D hand motion trajectory prediction, PBR Brain-Comp. Interf. Lab Exp. to Real-World Appl. Vol 228 (2016) 71–105.
[20] A. Korik, N. Siddique, R. Sosnik, D. Coyle, 3D hand movement velocity reconstruction using power spectral density of EEG signals and neural network, Proc. Annu. Int. Conf. IEEE Eng. Med. Biol. Soc. EMBS (2015) 8103–8106, https://doi.org/10.1109/EMBC.2015.7320274, 2015-Novem.
[21] N. Bernstein, The Co-Ordination and Regulation of Movements, Elsevier, 1967, https://doi.org/10.1016/j.dcn.2018.02.010.
[22] A. Bicchi, M. Gabiccini, M. Santello, Modelling natural and artificial hands with synergies, Philos. Trans. R. Soc. B Biol. Sci. 366 (2011) 3153–3161, https://doi.org/10.1098/rstb.2011.0152.
[23] R. Vinjamuri, M. Sun, C. Chang, H. Lee, R.J. Sclabassi, Dimensionality reduction in control and coordination of the Human hand, IEEE Trans. Biomed. Eng. 57 (2010) 284–295.
[24] M. Santello, G. Baud-bovy, H. Jörntell, Neural bases of hand synergies, Front. Comput. Neurosci. 7 (2013) 23, https://doi.org/10.3389/fncom.2013.00023.
[25] M.C. Tresch, P. Saltiel, E. Bizzi, The construction of movement by the spinal cord, Nat. Neurosci. 2 (1999) 162–167.
[26] R. Gentner, J. Classen, Modular organization of finger movements by the Human Central nervous system, Neuron 52 (2006) 731–742, https://doi.org/10.1016/j.neuron.2006.09.038.
[27] R. Vinjamuri, M. Sun, C. Chang, H. Lee, R.J. Sclabassi, Z. Mao, Temporal postural synergies of the hand in rapid grasping tasks, IEEE Trans. Technol. Biomed. 14 (2010) 986–994.
[28] T. Pistohl, A. Schulze-bonhage, A. Aertsen, C. Mehring, T. Ball, Decoding natural grasp types from human ECoG, Neuroimage 59 (2012) 248–260, https://doi.org/10.1016/j.neuroimage.2011.06.084.
[29] A. Leo, G. Handjaras, M. Bianchi, H. Marino, M. Gabiccini, A. Guidi, E.P. Scilingo, P. Pietrini, A. Bicchi, M. Santello, E. Ricciardi, A synergy-based hand control is encoded in human motor cortical areas, Elife 5 (2016) 1–32, https://doi.org/10.7554/eLife.13420.
[30] N. Jarrassé, T. Proietti, V. Crocher, J. Robertson, A. Sahbani, G. Morel, A. Roby-Brami, R. Ronsse, G. Sahbani, A. Morel, Robotic exoskeletons: a perspective for the rehabilitation of arm coordination in stroke patients, Front. Hum. Neurosci. 8 (2014) 947, https://doi.org/10.3389/fnhum.2014.00947.
[31] D. Pei, V. Patel, M. Burns, R. Chandramouli, R. Vinjamuri, Neural decoding of synergy-based hand movements using electroencephalography, IEEe Access. 7 (2019) 18155–18163, https://doi.org/10.1109/ACCESS.2019.2895566.
[32] D. Pei, P. Olikkal, T. Adali, R. Vinjamuri, Reconstructing synergy-based hand grasp kinematics from electroencephalographic signals, Sensors 22 (2022), https://doi.org/10.3390/s22145349.
[33] A. Guillot, C. Collet, Contribution from neurophysiological and psychological methods to the study of motor imagery, Brain Res. Rev. 50 (2005) 387–397, https://doi.org/10.1016/j.brainresrev.2005.09.004.
[34] M. Jeannerod, J. Decety, Mental motor imagery: a window into the representational stages of action, Curr. Opin. Neurobiol. 5 (1995) 717–732.
[35] S. Hétu, M. Grégoire, A. Saimpont, M.P. Coll, F. Eugène, P.E. Michon, P.L. Jackson, The neural network of motor imagery: an ALE meta-analysis, Neurosci. Biobehav. Rev. 37 (2013) 930–949, https://doi.org/10.1016/j.neubiorev.2013.03.017.
[36] G. Abbruzzese, C. Trompetto, M. Schieppati, The excitability of the human motor cortex increases during execution and mental imagination of sequential but not repetitive finger movements, Exp. Brain Res. 111 (1996) 465–472.
[37] J. Decety, Do imagined and executed actions share the same neural substrate? Cogn. Brain Res. 3 (1996) 87–93.
[38] W.H. Lee, E. Kim, H.G. Seo, B.M. Oh, H.S. Nam, Y.J. Kim, H.H. Lee, M.G. Kang, S. Kim, M.S. Bang, Target-oriented motor imagery for grasping action: different characteristics of brain activation between kinesthetic and visual imagery, Sci. Rep. 9 (2019) 1–14, https://doi.org/10.1038/s41598-019-49254-2.
[39] V. Patel, M. Burns, D. Pei, R. Vinjamuri, V. Patel, M. Burns, R. Chandramouli, R. Vinjamuri, Neural decoding of synergy-based hand movements using electroencephalography, IEEe Access. 7 (2019) 18155–18163, https://doi.org/10.1109/ACCESS.2019.2895566.
[40] H. Agashe, J.L. Contreras-Vidal, Reconstructing hand kinematics during reach to grasp movements from electroencephalographic (EEG) signals, in: 33rd annu. Int. Conf, IEEE EMBS (2011) 5444–5447.
[41] A. Perry, S. Bentin, Mirror activity in the human brain while observing hand movements: a comparison between EEG desynchronization in the μ-range and previous fMRI results, Brain Res. 1282 (2009) 126–132, https://doi.org/10.1016/j.brainres.2009.05.059.
[42] T. Hayashi, H. Yokoyama, I. Nambu, Y. Wada, Prediction of individual finger movements for motor execution and imagery : an EEG study, 2017 IEEE Int. Conf. Syst. Man, Cybern (2017) 3020–3023, https://doi.org/10.1109/SMC.2017.8123088.
[43] H.C. Kwan, Spatial organization of Precentrd cortex in Awake primates . II . Motor outputs, J. Neurophysiol. 41 (1978) 1120–1131, https://doi.org/10.1152/jn.1978.41.5.1120.
[44] B.J. McKiernan, J.K. Marcario, J.H. Karrer, P.D. Cheney, Corticomotoneuronal postspike effects in shoulder, elbow, wrist, digit, and intrinsic hand muscles during a reach and prehension task, J. Neurophysiol. 80 (2018) 1961–1980.
[45] M.C. Park, A. Belhaj-saı, M. Gordon, P.D. Cheney, Consistent features in the forelimb representation of primary motor cortex in Rhesus macaques, J. Neurophysiol. 21 (2001) 2784–2792.
[46] J.A. Rathelot, P.L. Strick, Muscle representation in the macaque motor cortex: an anatomical perspective, Proc. Natl. Acad. Sci 103 (2006) 8257–8262, https://doi.org/10.1073/pnas.0602933103.
[47] S. Acharya, M.S. Fifer, H.L. Benz, N.E. Crone, N.V. Thakor, Electrocorticographic amplitude predicts finger positions during slow grasping motions of the hand, J. Neural Eng. 7 (2010) 046002, https://doi.org/10.1088/1741-2560/7/4/046002.
[48] V. Patel, M. Burns, D. Pei, R. Vinjamuri, Decoding synergy-based hand movements using electroencephalography, 40th Annu. Int. Conf. IEEE Eng. Med. Biol. Soc. (2018) 4816–4819.
[49] G. Torres-Oviedo, L.H. Ting, Subject-specific muscle synergies in human balance control are consistent across different biomechanical contexts, J. Neurophysiol. 103 (2010) 3084–3098, https://doi.org/10.1152/jn.00960.2009.
[50] A. D'Avella, E. Bizzi, Shared and specific muscle synergies in natural motor behaviors, Proc. Natl. Acad. Sci. U. S. A. 102 (2005) 3076–3081, https://doi.org/10.1073/pnas.0500199102.
[51] B. Xu, Y. Wang, L. Deng, C. Wu, W. Zhang, H. Li, A. Song, Decoding hand movement types and kinematic information from electroencephalogram, IEEE Trans. Neural Syst. Rehabil. Eng. 29 (2021) 1744–1755, https://doi.org/10.1109/TNSRE.2021.3106897.
[52] H.S. Lee, L. Schreiner, S. Jo, S. Sieghartsleitner, M. Jordan, H. Pretl, C. Guger, H. Park, Individual finger movement decoding using a novel brain-computer interface system, Front. Neurosci. 8 (2022) 1–16, https://doi.org/10.3389/fnins.2022.1009878.
[53] R. Meattini, R. Suárez, S. Member, G. Palli, S. Member, C. Melchiorri, Human to robot hand motion mapping methods : review and classification, IEEE Trans. Robot. 39 (2023) 842–861, https://doi.org/10.1109/TRO.2022.3205510.
[54] H. Yuan, C. Perdoni, B. He, Relationship between speed and EEG activity during imagined and executed hand movements, J. Neural Eng. 7 (2010) 026001.
[55] D.J. McFarland, L.A. Miner, T.M. Vaughan, J.R. Wolpaw, Mu and beta rhythm topographies during motor imagery and actual movements, Brain Topogr. 12 (2000) 177–186, https://doi.org/10.1023/A:1023437823106.
[56] G. Pfurtscheller, A. Stancák, G. Edlinger, On the existence of different types of central beta rhythms below 30 hz, Electroencephalogr. Clin. Neurophysiol. 102 (1997) 316–325, https://doi.org/10.1016/S0013-4694(96)96612-2.
[57] L. Li, J. Wang, G. Xu, M. Li, J. Xie, The study of object-oriented motor imagery based on EEG suppression, PLoS. One 10 (2015) 1–10, https://doi.org/10.1371/journal.pone.0144256.
[58] M.G. Lacourse, E.L.R. Orr, S.C. Cramer, M.J. Cohen, Brain activation during execution and motor imagery of novel and skilled sequential hand movements, Neuroimage 27 (2005) 505–519, https://doi.org/10.1016/j.neuroimage.2005.04.025.
[59] M. Matsuo, N. Iso, K. Fujiwara, T. Moriuchi, D. Matsuda, W. Mitsunaga, A. Nakashima, T. Higashi, Comparison of cerebral activation between motor execution and motor imagery of self-feeding activity, Neural Regen. Res. 16 (2021) 778–782, https://doi.org/10.4103/1673-5374.295333.
[60] P. Ofner, G.R. Müller-Putz, Using a noninvasive decoding method to classify rhythmic movement imaginations of the arm in two planes, IEEE Trans. Biomed. Eng. 62 (2015) 972–981, https://doi.org/10.1109/TBME.2014.2377023.
[61] R. Prevete, F. Donnarumma, A. D'Avella, G. Pezzulo, Evidence for sparse synergies in grasping actions, Sci. Rep. 8 (2018) 1–16, https://doi.org/10.1038/s41598-017-18776-y.
[62] R. Vinjamuri, Z. Mao, R.J. Sclabassi, C. Diagnostics, M. Sun, Time-varying synergies in velocity profiles of finger joints of the hand during reach and grasp, in: 29th Annu. Int. Conf. IEEE EMBS (2007) 4846–4849, https://doi.org/10.1109/IEMBS.2007.4353425.
[63] V. Gracia-Ibáñez, J.L. Sancho-Bru, M. Vergara, N.J. Jarque-Bou, A. Roda-Sales, Sharing of hand kinematic synergies across subjects in daily living activities, Sci. Rep. 10 (2020) 1–11, https://doi.org/10.1038/s41598-020-63092-7.
[64] R.M.AA da Silva Costa, T. Hortobágyi, R. den Otter, A. Sawers, Age, cognitive task, and arm position differently affect muscle synergy recruitment but have similar effects on walking balance, Neuroscience 527 (2023) 11–21.
[65] C.N.R Macchi, A. Santuz, A. Hays, F. Vercruyssen, A. Arampatzis, A Bar-Hen, sex influence on muscle synergies in a ballistic force-velocity test during the delayed recovery phase after a graded endurance run, Heliyon. 8 (2022).
[66] G. Bartur, H. Pratt, N. Soroker, Changes in mu and beta amplitude of the EEG during upper limb movement correlate with motor impairment and structural damage in subacute stroke, Clin. Neurophysiol. 130 (2019) 1644–1651, https://doi.org/10.1016/j.clinph.2019.06.008.
[67] J.A. Barios, S. Ezquerro, A. Bertomeu-Motos, J.M. Catalan, J.M. Sanchez-Aparicio, L. Donis-Barber, E. Fernandez, N. Garcia-Aracil, Movement-related EEG oscillations of contralesional hemisphere discloses compensation mechanisms of severely affected motor chronic stroke patients, Int. J. Neural Syst. (2021) 31, https://doi.org/10.1142/S0129065721500532.
[68] M. Bönstrup, L. Krawinkel, R. Schulz, B. Cheng, J. Feldheim, G. Thomalla, L. G. Cohen, C. Gerloff, Low-frequency brain oscillations track motor recovery in Human stroke, Ann. Neurol. 86 (2019) 853–865, https://doi.org/10.1002/ana.25615.
[69] A.R. Anwar, M. Muthalib, S. Perrey, A. Galka, O. Granert, S. Wolff, U. Heute, G. Deuschl, J. Raethjen, M. Muthuraman, Effective connectivity of cortical sensorimotor networks during finger movement tasks: a simultaneous fNIRS, fMRI, EEG study, Brain Topogr. 29 (2016) 645–660, https://doi.org/10.1007/s10548-016-0507-1.
[70] C. Chen, J. Zhang, A.N. Belkacem, S. Zhang, R. Xu, B. Hao, Q. Gao, D. Shin, C. Wang, D. Ming, G-causality brain connectivity differences of finger movements between motor execution and motor imagery, J. Healthc. Eng 2019 (2019) 1–13, https://doi.org/10.1155/2019/5068283.
[71] V. Kaiser, I. Daly, F. Pichiorri, D. Mattia, G.R. Müller-Putz, C. Neuper, Relationship between electrical brain responses to motor imagery and motor impairment in

stroke, Stroke 43 (2012) 2735–2740, https://doi.org/10.1161/STROKEAHA.112.665489.
[72] M. Butt, G. Naghdy, F. Naghdy, G. Murray, H. Du, Investigating the detection of intention signal during different exercise protocols in robot-assisted hand movement of stroke patients and healthy subjects using EEG-BCI system, Adv. Sci. Technol. Eng. Syst. 4 (2019) 300–307, https://doi.org/10.25046/aj040438.
[73] A.E. Voinas, R. Das, M.A. Khan, I. Brunner, S. Puthusserypady, Motor imagery EEG signal classification for Stroke Survivors rehabilitation, Int. Winter Conf. Brain-Computer Interface, BCI (2022) 1–5, https://doi.org/10.1109/BCI53720.2022.9734837, 2022-Febru.
[74] H. Raza, A. Chowdhury, S. Bhattacharyya, Deep learning based prediction of EEG motor imagery of stroke patients' for neuro-rehabilitation application, in: Proc. Int. Jt. Conf. Neural Networks, 2020, pp. 0–7, https://doi.org/10.1109/IJCNN48605.2020.9206884.
[75] R.R. Lu, M.X. Zheng, J. Li, T.H. Gao, X.Y. Hua, G. Liu, S.H. Huang, J.G. Xu, Y. Wu, Motor imagery based brain-computer interface control of continuous passive motion for wrist extension recovery in chronic stroke patients, Neurosci. Lett. 718 (2020) 1–8, https://doi.org/10.1016/j.neulet.2019.134727.
[76] M. Spüler, E. López-Larraz, A. Ramos-Murguialday, On the design of EEG-based movement decoders for completely paralyzed stroke patients, J. Neuroeng. Rehabil. 15 (2018) 1–12, https://doi.org/10.1186/s12984-018-0438-z.